PPPL Seminar, 28th February 2011

Recent MAST Results & Plans

Anthony Field

EURATOM / CCFE Fusion Association

CCFE is the fusion research arm of the **United Kingdom Atomic Energy Authority**

Jointly funded by EURATOM & RCUK Energy Programme

Outline

- Introduction
- Recent MAST results and plans
  - ELM and pedestal physics
  - Exhaust physics
  - Confinement and transport
  - Stability
  - Current drive and profile optimisation
- MAST Upgrade
- Summary

CCFE re-organisation

- Tokamak science programme:
  - Squeeze on EPSRC funded science (cost of MAST-U, reduced EU contribution) necessitates implementing austerity measures
  - More efficient, cross-site management of science programme
  - Separate management of MAST-U project, ITER systems, etc.
- Five new Programme Leaders (3-years to March 2014):
  - Integrated Operational Scenarios: C. Challis, M. Romanelli
  - Core plasma: I. Chapman, S. Pinches, D. McDonald, M. Valovic
  - SOL and Divertor: W. Fundamenski
- Facilities/Infrastructure managers (FMs)
  - MAST – B. Lloyd
  - Theory and Modelling – T. Hender
  - JET participation – A. W. Morris
  - Fusion Programme Manager – M. O'Brien

MAST Mission

- To explore the long term potential of the spherical tokamak as a fusion component test facility (CTF) and/or ST power plant (STPP):

  Driven primarily by needs for an ST-based Component Test Facility (CTF), e.g. confinement scaling + potential show-stoppers (e.g. non-solenoid start-up, current drive, exhaust…). Input from IEA-IA on Spherical Tori + MAST PAC etc

- To advance key tokamak physics for optimal exploitation of ITER and DEMO design optimisation:

  EFDA WP, ITPA high priority R & D, IEA – ITPA co-ordinated experiments, ITPA Topical Group Work plans + MAST PAC etc

- To provide unique insight into underlying tokamak physics:

  Strong underlying physics programme essential to engage university interest. Extreme characteristics (e.g. high beta, toroidicity, & flow shear; super-Alfvenic ions etc.), backed up by a comprehensive suite of high resolution diagnostics

MAST operating schedule I

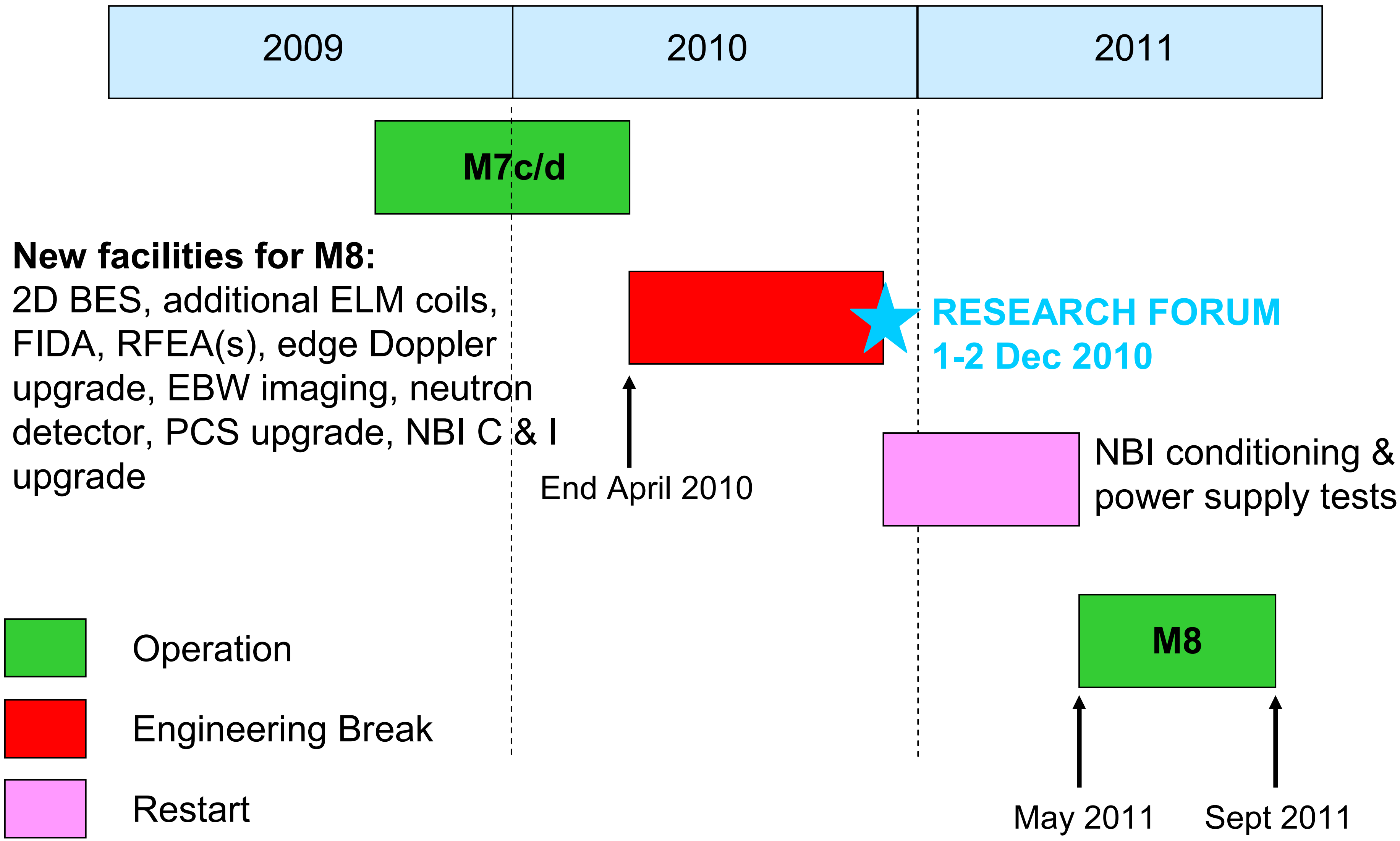

MAST operations 2011-13

- Considerable fraction of resources redirected to MAST-U
- MAST operation limited to 6 months/year 2011-13 (timing optimised to JET and MAST-U requirements)
- Aim to operate during 2011-13 without a major vent (very limited new enhancements)
- Prioritise engineering activities for MAST-U relevance:
  - Modified sliding joint tests (M8)
  - Fast-amplifier tests (vertical stability)
  - NBI system developments (arc-ripple, DECEL, etc)
  - HVPS-5 commissioning and tests
  - Long-pulse DATAQ commissioning

Recent MAST enhancements

- Additional ELM control coils: 6 + 12 internal array (n = 3, 4, 6)
- TAE antennae: active excitation with increased resonant drive circuit
- TS upgrade: + smart triggering system (synchronised to pellets, NTMs etc)
- Multi-channel MSE: now 37 spatial channels, better than 3 cm, 2 ms resolution
- Edge Doppler upgrade: high frequency velocity ($v_{\phi,\theta}$) fluctuations EFDA task
- 2D BES: long wavelength turbulence (with RMKI Hungary) EFDA task
- Fast Ion D-Alpha (FIDA): fast ion distribution EFDA task
- Collimated neutron detector: fast ion distribution (with Uppsala Univ.) EFDA task
- EBW emission imaging: edge j(r) measurement (York University) EPSRC grant
- Retarding field energy analyzer(s) for SOL Ti: outboard mid-plane and divertor
- Disruption mitigation: MGI using fast gas valve (with FZJ)
- Divertor science facility with RFEA, spark-gap injector: (*DCU, Liverpool University*)
- Controllable HFS gas puffing system

ELM control

A Kirk et al

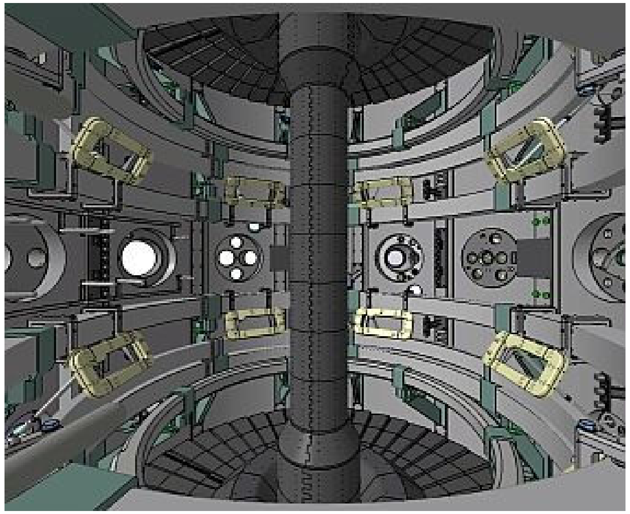

6+6 internal array: $\leq$ 1.4 kA, 4-turn coils (n = 3)
- similar to DIII-D I-coils

Even parity
(Same sign current in upper and lower coils at same toroidal location)

I_{coil}^{up} + - + - + -
I_{coil}^{down} + - + - + -

Odd parity
(Opposite sign current in upper and lower coils at same toroidal location)

I_{coil}^{up} + - + - + -
I_{coil}^{down} - + - + - +

- Resonant effects observed in L-mode with similar I_{coil} threshold (~ 1kA)
  - density pump-out
  - enhanced fluctuations (inside LCFS)
  - increased (more positive) E_r^{ped}
- ELMs triggered in ELM-free discharges or type-III ELM frequency increased
- Initially no effect on type I ELMs observed despite $\sigma_{chir} > 1$
- Type I ELM mitigation subsequently observed if q_{95} carefully optimised

Mitigation of type-I ELMs

A Kirk et al

- q scan to find 'optimum' alignment with applied perturbation
- Chirikov parameter little changed but resonant field changes

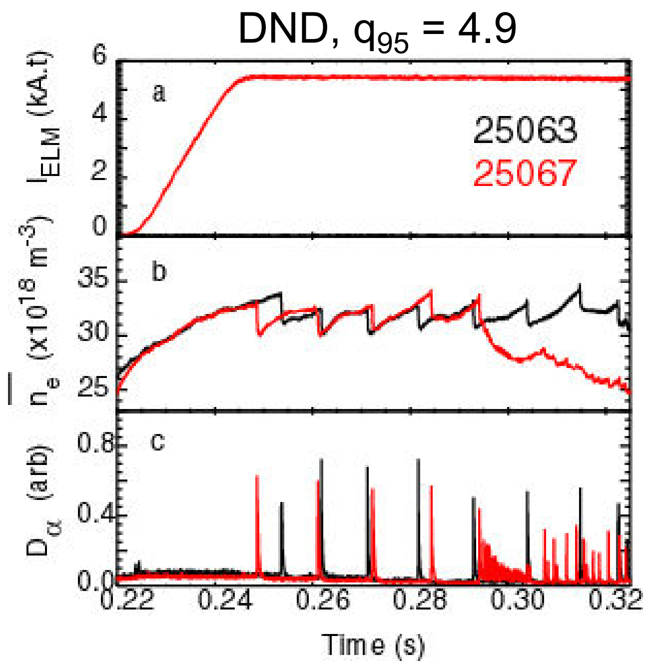

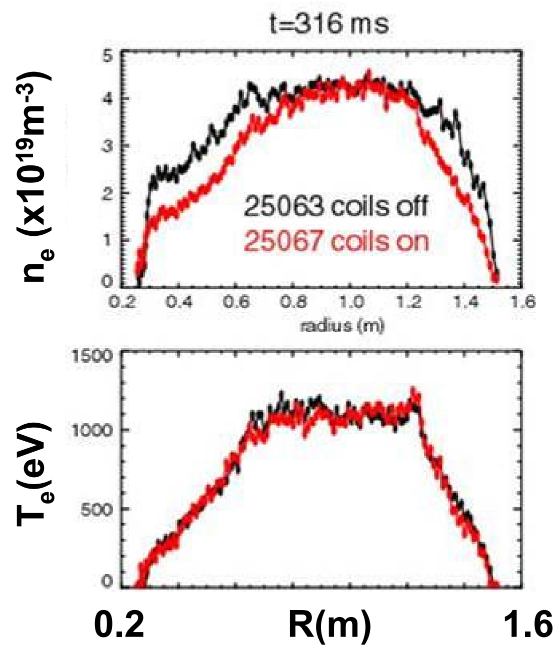

Strong effect on density

Little effect on T_e

- f_{ELM} increases by 5, ΔW_{ELM} reduces from 5 kJ to ~ 1kJ (f_{ELM}. ΔW_{ELM} ~ constant)
- W_{MHD} reduced by ~ 8%
- Pedestal parameters suggest transition from type I to type IV ELMs (low ν* type-III)
- ELM mitigation also observed in SN discharges

CCFE CULHAM CENTRE FOR FUSION ENERGY

Plasma response (L-mode)

A Kirk et al

- Pump-out different between even and odd parity discharges with similar alignment and Chirikov parameter
  - → Chirikov not the only important parameter
  - → Resonant component of applied field different

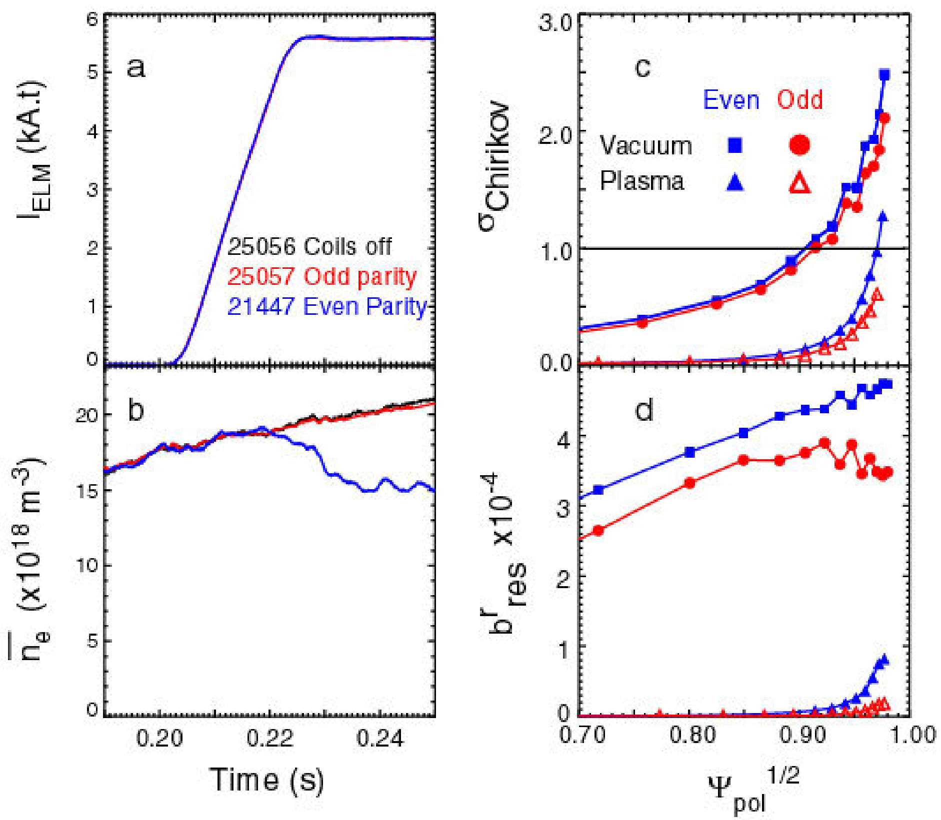

MARS-F:

- single-fluid, linear MHD code
- solves full resistive MHD equations in toroidal geometry
- takes into account plasma response and screening due to toroidal rotation

Results:

- Large reduction of resonant components
- Smaller reduction in Chirikov parameter
- Enhances relative difference in b^r_{res} between even and odd parity

M8 exploit additional lower ECC

A Kirk et al

- Allows n=4 and n=6 configurations and better alignment to q_{95}~ 5 discharges
- Higher 'figure of merit' for magnetic perturbation spectrum

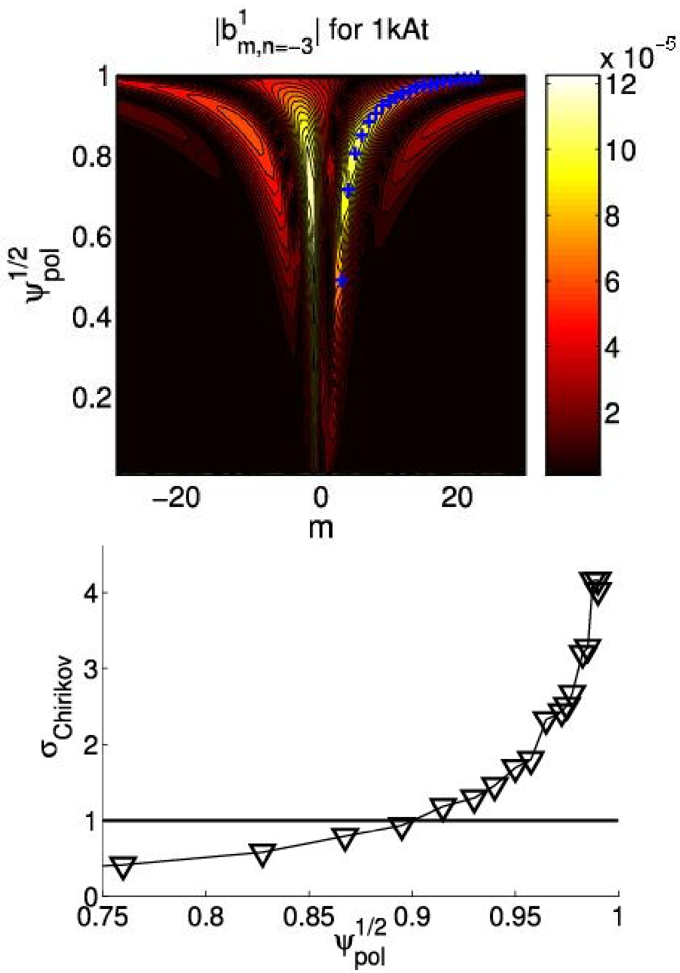

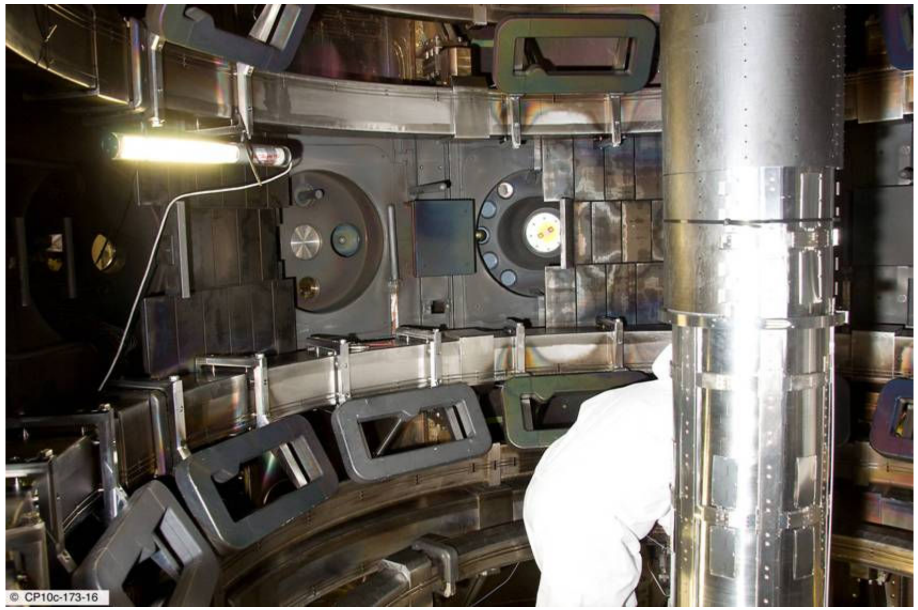

Pedestal – edge $T_i(r)$ measurements

Edge T_i measurements

- Novel high resolution edge T_i measurements from CX emission of C^{6+}
- Utilises localised, cold deuterium gas puff to localize measurement

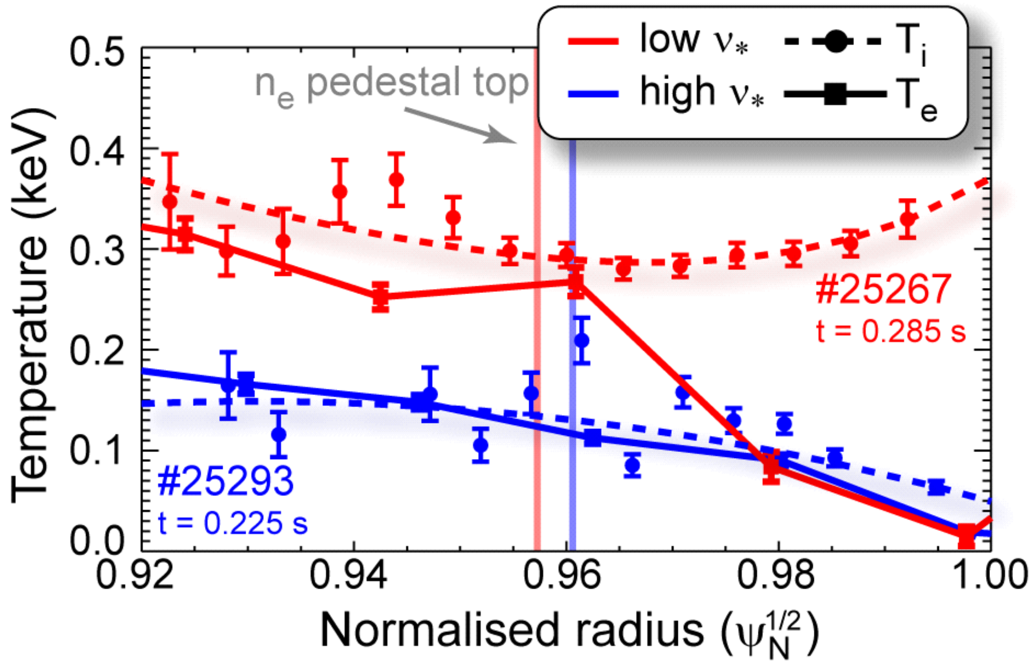

- Collisionality dependence consistent with analysis of Kagan & Catto PPCF **50**, 085010 (2008), which showed that in the banana regime $L_{Ti} >> \rho_{i,pol}$

Pedestal – edge j(r) measurements

- Large magnetic field line tilt in the ST enables MSE measurements of edge $j_\phi(r)$ evolution with 2ms resolution

- Small effect of measured radial electric field included
- Large increase in edge current density at L-H transition (x5)
- ELITE calculations show pedestal in vicinity of ballooning stability boundary at time of type-I ELMs
- Time-dependence of j_ϕ, ∇p exhibit unexplained features

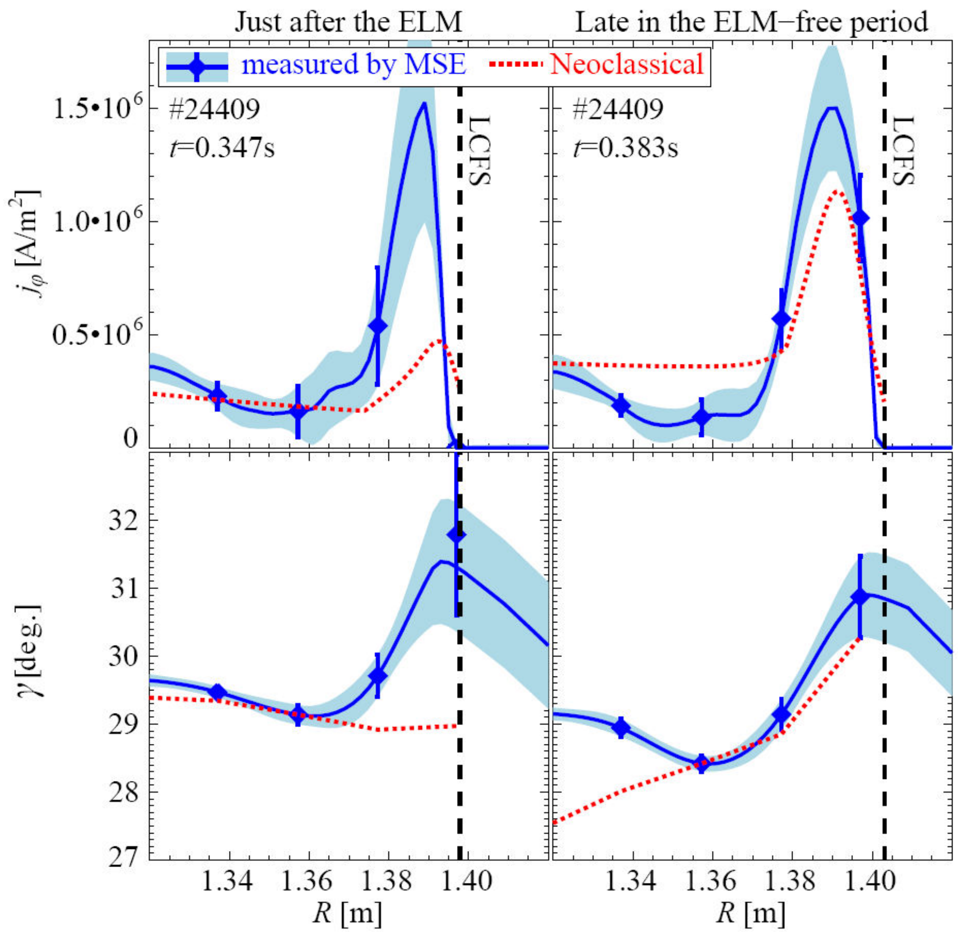

M. De Bock, H. Meyer et al

EBW emission measurements of $j_\phi(r)$

ELM/Pedestal	Exhaust	Conf/transport	Stability	CD/profile opt.

- EBW measurements with a fast spinning mirror ($\Delta t \sim 10ms$)
- Indicates large localized magnetic field line tilt angle changes at the plasma edge in ELM-free H-mode
- Implies bi-directional radial current structure near the LCFS (cf. ELM model of Gimblett et al PRL 2006)

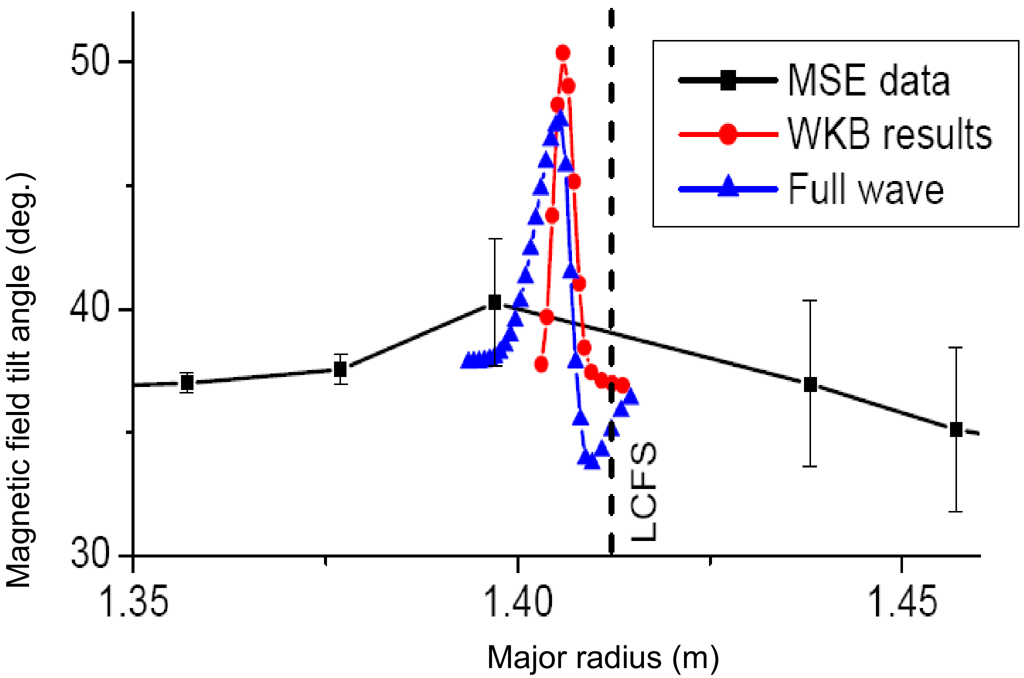

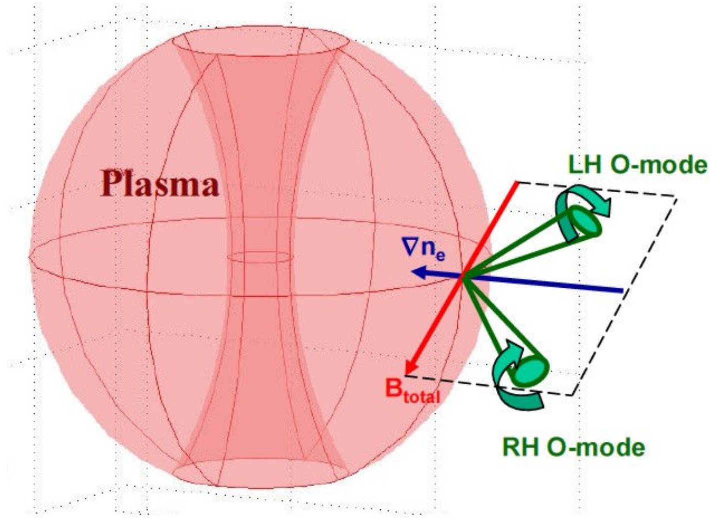

$\sin^2\phi = N^2_{\|,opt} = Y/(Y+1), \quad Y = \omega_{ce}/\omega$

2D EBW imaging system

- Phased array antenna of 37 miniature ‘Vivaldi’ antennas
- 8 antennae connected at a time
- 20 μs time resolution (ELM cycle)
- 16 frequency channels from 10-35GHz
- Full vector heterodyne down-conversion
- IF digitised by high bandwidth FPGA

Heterodyne receiver

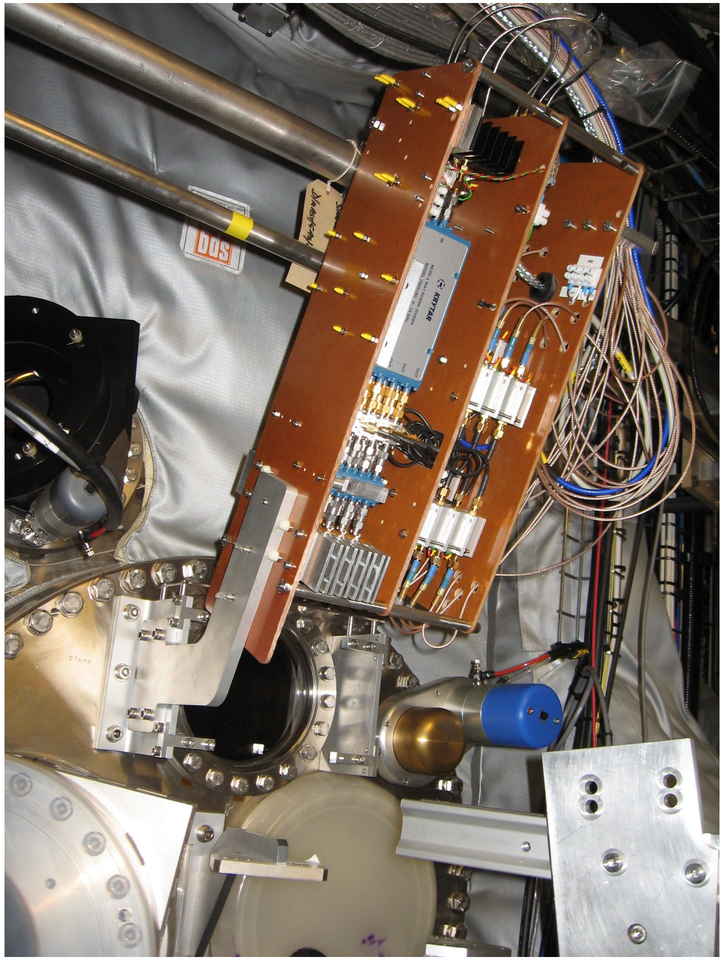

Phased array antenna

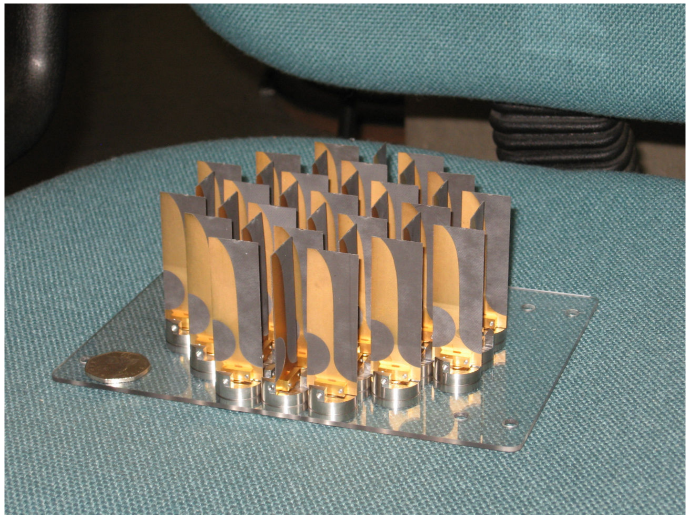

V. Shevchenko, S Freethy, R Vann

Edge Doppler spectroscopy upgrade

Fast CCD detectors

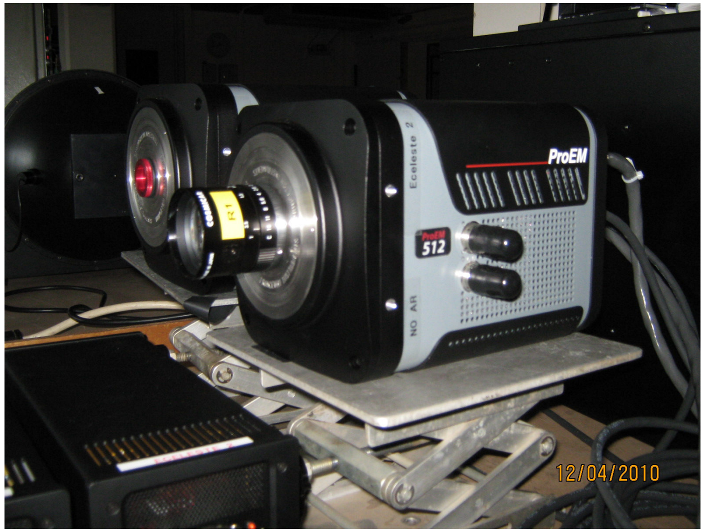

Fast piezo valve (200 Hz) in nozzle

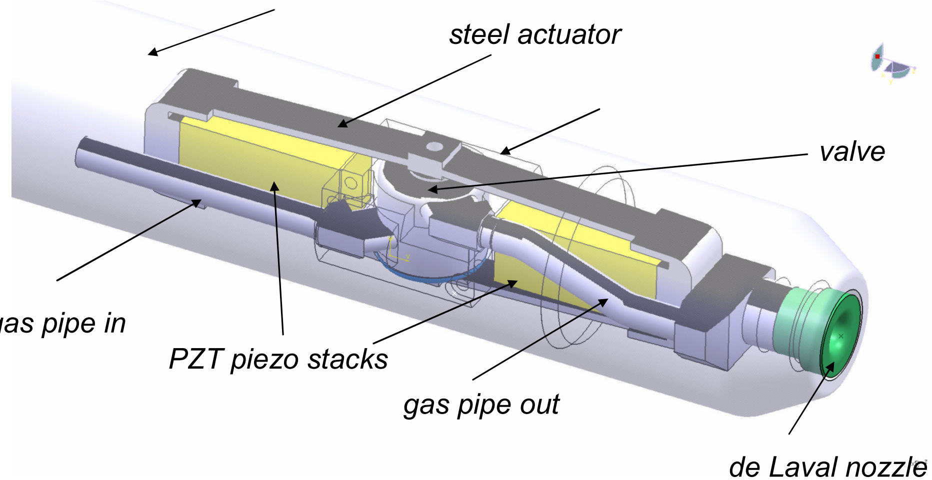

E-CELESTE upgrade:

- New fast CCD detectors (≤ 50 KHz)
- Modulated gas nozzle (200 Hz) to facilitate background subtraction
- Higher étendu collection optics (increased from F/7 to F/2) for increased sensitivity

Capabilities:

- Simultaneous measurement of $v_{i\theta}$, $v_{i\phi}$, E_r, and T_i
- Measurements at frequencies covering the GAM range (~ 10 KHz)

EFDA Task

H. Meyer et al

SOL ion energy measurements

Motivation:

- Data useful for interpretation of probe data (n_e, P_{div})
- Determines physical sputtering rates from plasma facing materials
- ELM ion energies in the far SOL are unknown

- First measurements show $T_i \sim (1 – 2.6)\times T_e$ at LFS mid-plane
- High ion energies (> 500 eV) during ELM filaments up to 20cm from the LCFS

Retarding Field Analyzer (CEA)

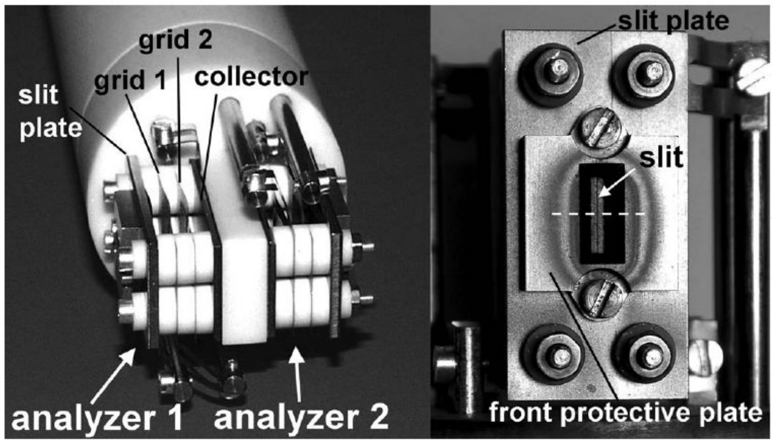

RFEA supplied by CEA Cadarache

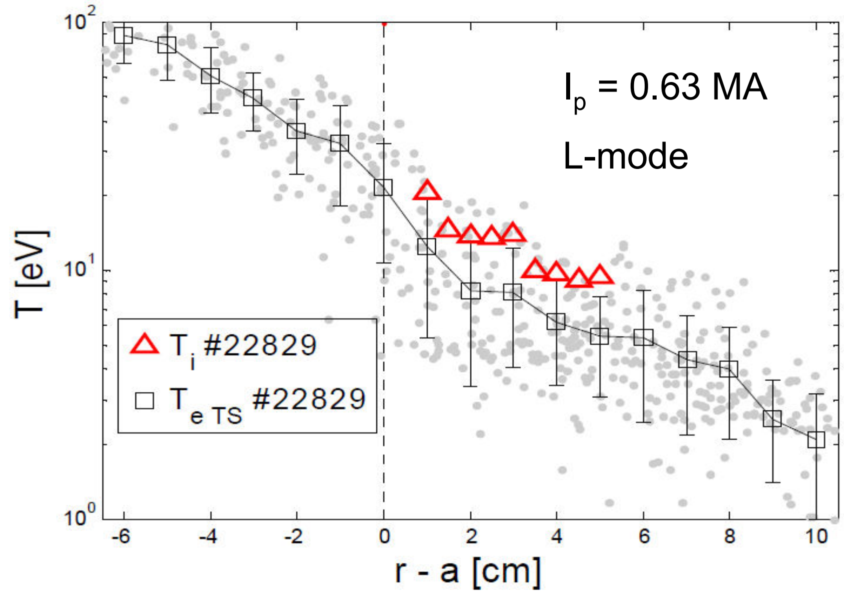

P. Tamain, S. Allan, S. Elmore (Liverpool U.)

Disruption mitigation

- Radiation enhancement by massive injection of 10^{22} particles (10% Ar, 90% He)

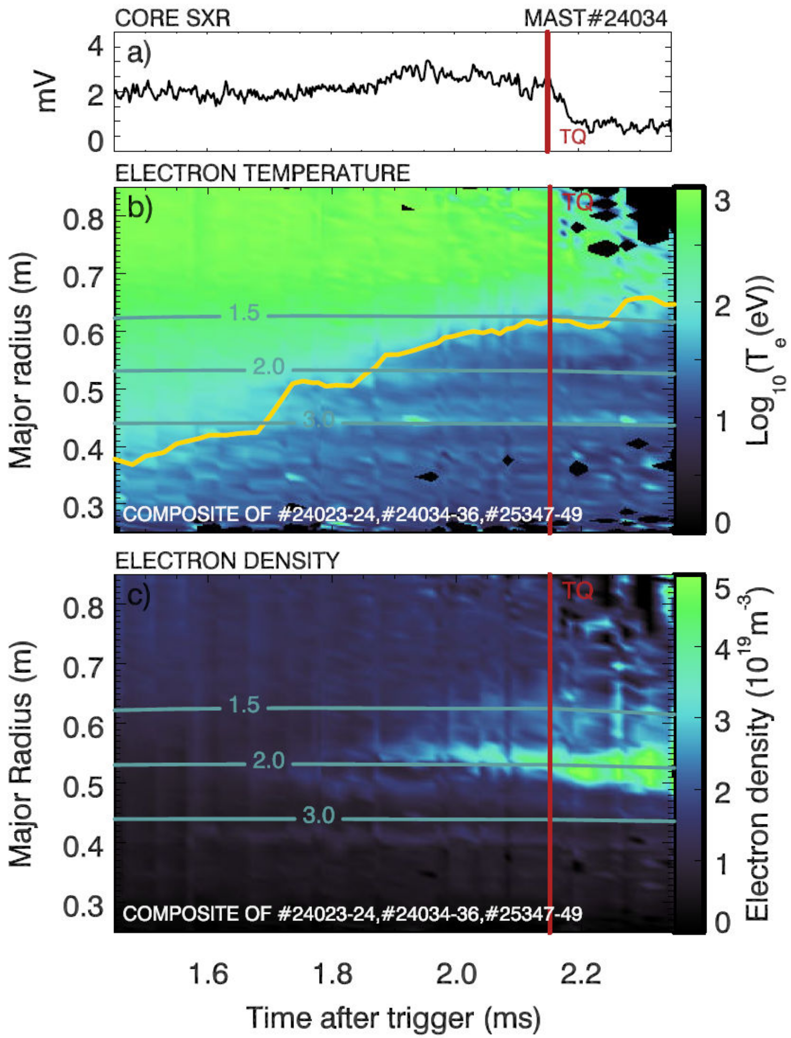

- Impurity ions penetrate to q = 2 surface prior to thermal quench (high speed imaging)
- Local density build-up and initiation of thermal quench when cool front reaches q = 2 surface

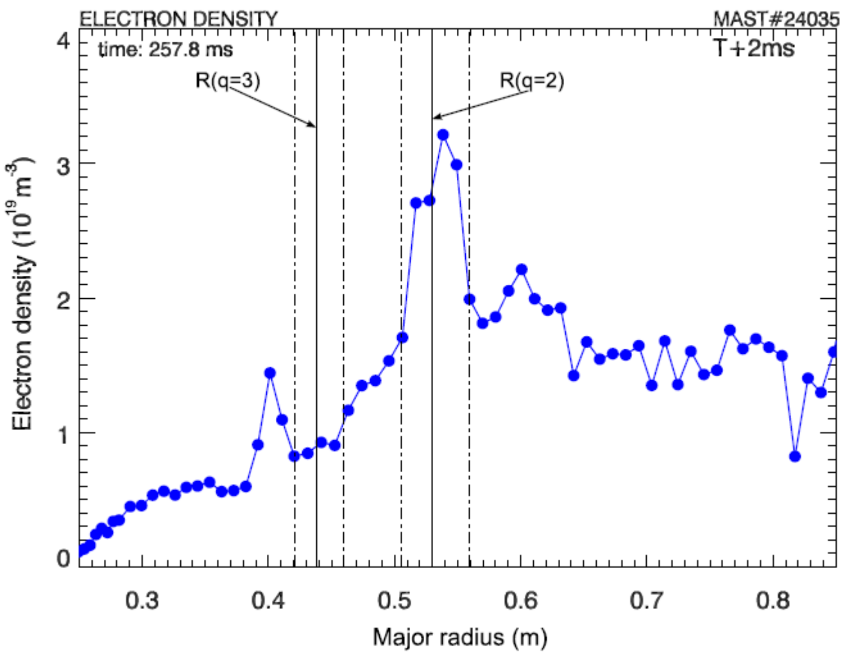

- 60–70% reduction in peak divertor power loads

Confinement scaling (ν^*, q)

ELM/Pedestal	Exhaust	Conf/transport	Stability	CD/profile opt.

- Dedicated scans: $\tau_{E,th}B_t \propto \nu_e{*}^{-0.82\pm0.1}q^{-0.85\pm0.2}$ cf. IPB98y2 $\tau_{E,th}B_t \propto \nu_e{*}^{0}q^{-3}$
- Consistent with reported dependence on engineering parameters $\tau_{E,th} \propto I_p^{0.6}B_t^{1.4}$

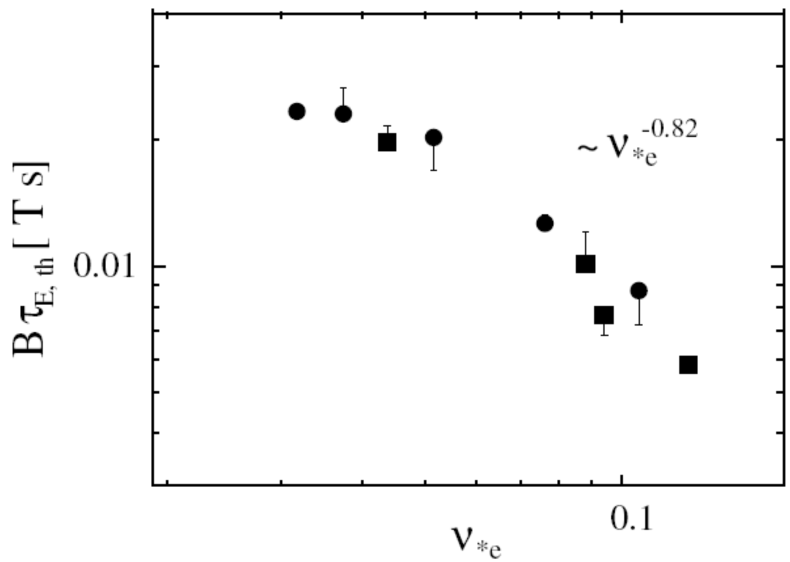

GYRO: micro-tearing modes might be a candidate to explain ν^*_e dependence

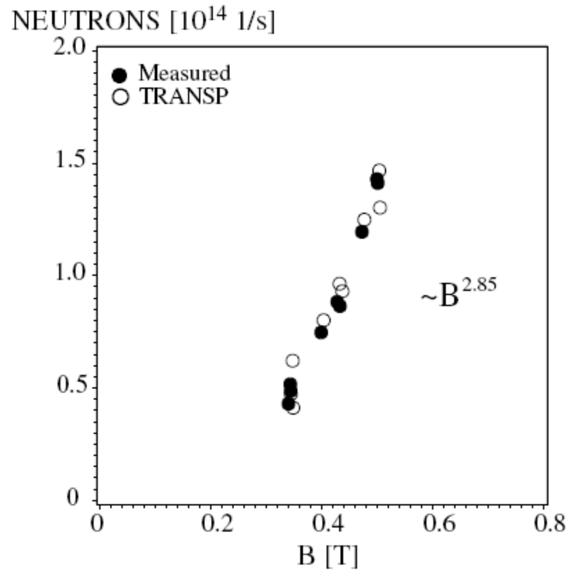

B_T dependence of neutron emission consistent with ν^* scaling

$$S_{DD} \propto B^{4x_\nu+6},\ B_T\tau_{E,th} \propto \nu_*^{x_\nu}$$

- ν^*_e scaling is important as largest extrapolation towards an ST-based CTF

ν* scan – transport analysis

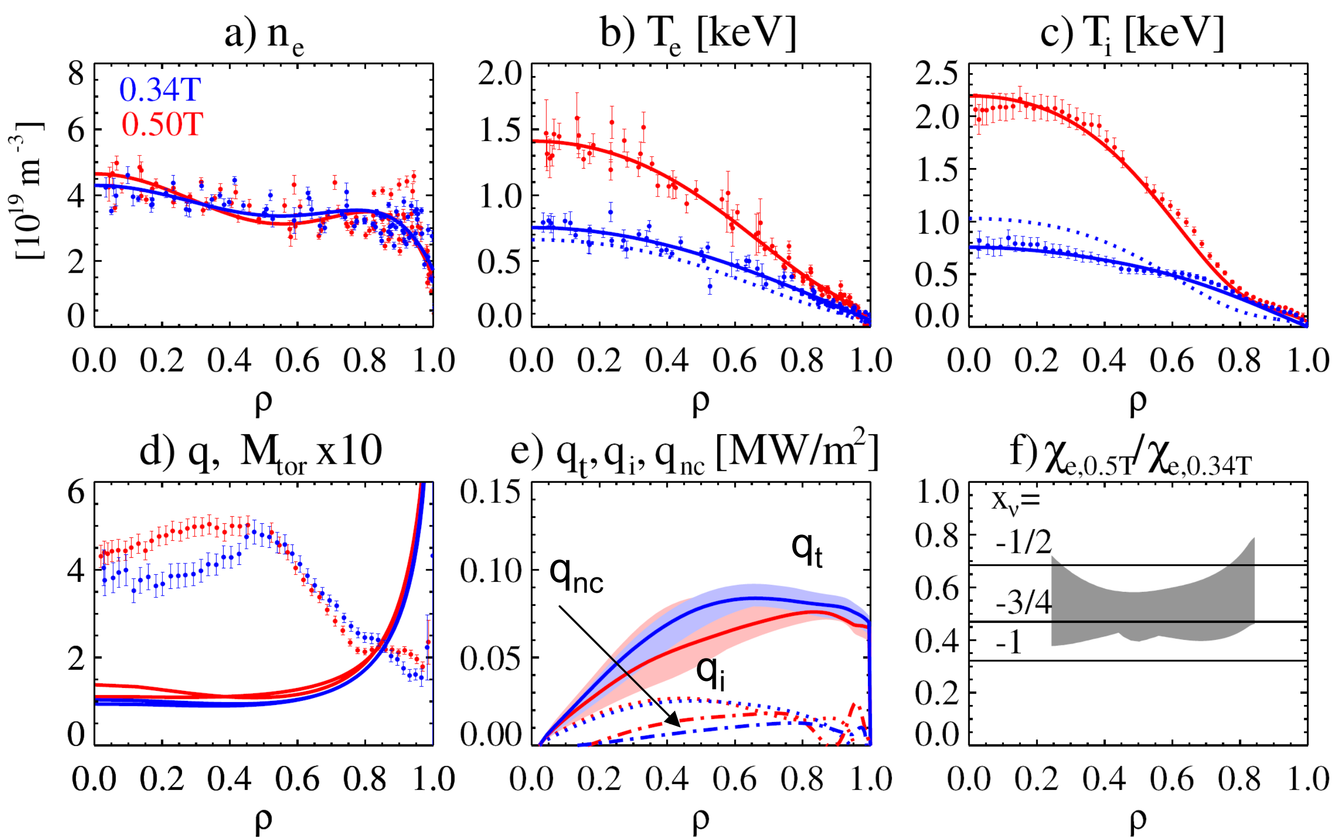

TRANSP

- Ion transport close to neo-classical, local heat transport dominated by electrons
- Necessary to assume $D_{FI} \leq 3$ m^2/s in TRANSP to match the measured neutron rate]
- Scaling of thermal diffusivity $\chi_e/B_t \propto \nu_e^{*(0.5 - 1)}$ consistent with global scaling

ITB formation studies

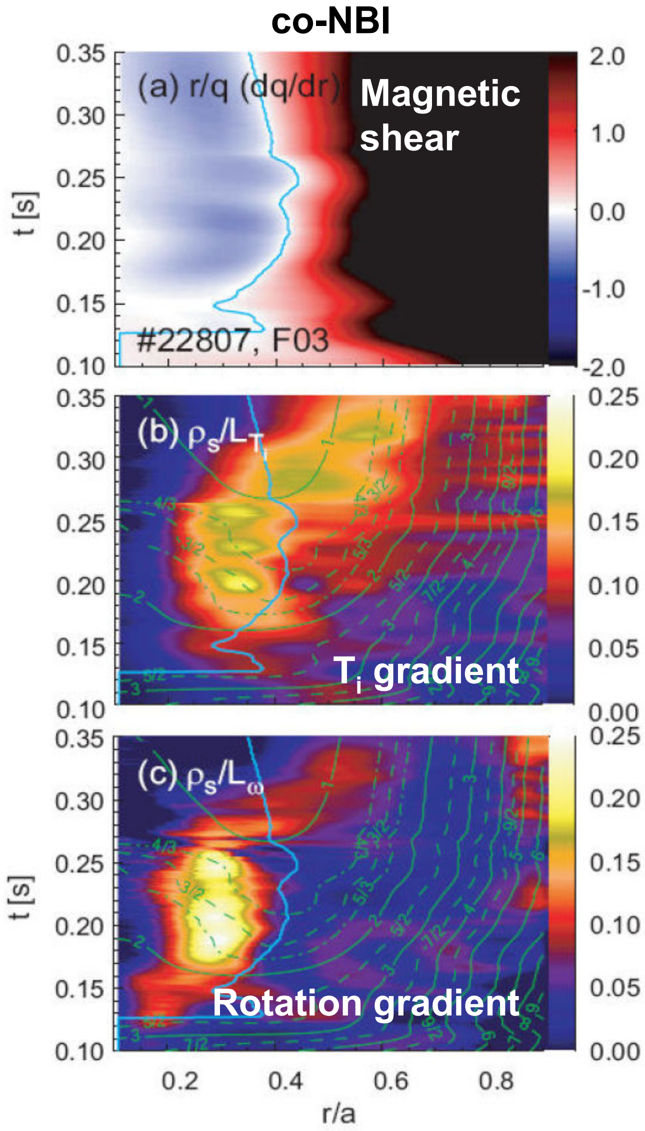

- MSE/CXRS enable influence of q(r) and flow shear on ITB formation to be studied
- Poloidal rotation is small – profiles consistent with neo-classical predictions
- Strong toroidal rotation dominates ExB flow shear
- H-mode: χ_i ~ 1-3 × χ_i^{NC} over most of radius
- L-mode: $\chi_i >> \chi_i^{NC}$ at large radius, but ion transport strongly suppressed by flow shear at mid-radius
- ITB formation favoured by early NBI → negative magnetic shear in the core
- With co-NBI, ITBs form in ion and momentum channels just inside q_{min} and $\chi_i \rightarrow \chi_i^{NC}$
- Some correlation between magnitude of r/Lw and the passing of q_{min} through rational values

ITB formation: micro-stability

- Linear, GS2 calculations with kinetic electrons performed with/without flow shear

  ρ = 0.3 (core): linearly stable to all modes with/without flow shear due to weak negative magnetic shear (result unchanged by inclusion of e.m. effects)

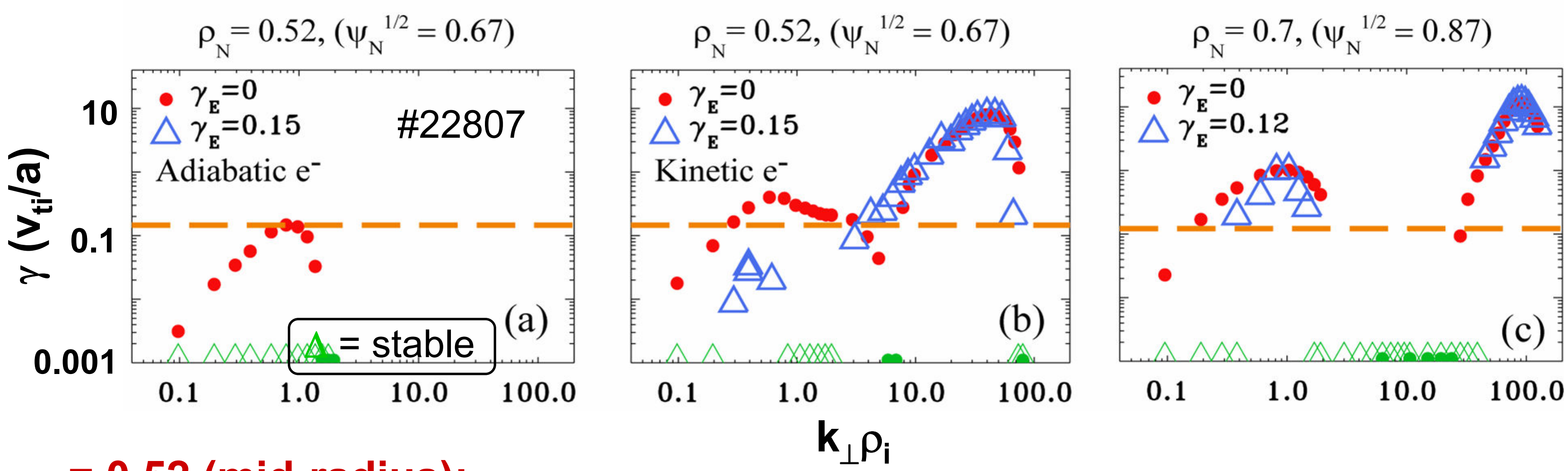

ρ = 0.52 (mid-radius):

- Adiabatic electrons – ITG modes fully stabilised by flow shear
- Kinetic electrons – appreciable TEM drive, only partially stabilised by flow shear

ρ = 0.7 (outer region):

- Weak flow shear insufficient to stabilise strongly growing ITG modes
- TEM modes stable due to reduced drive at higher collisionality

BES turbulence imaging system

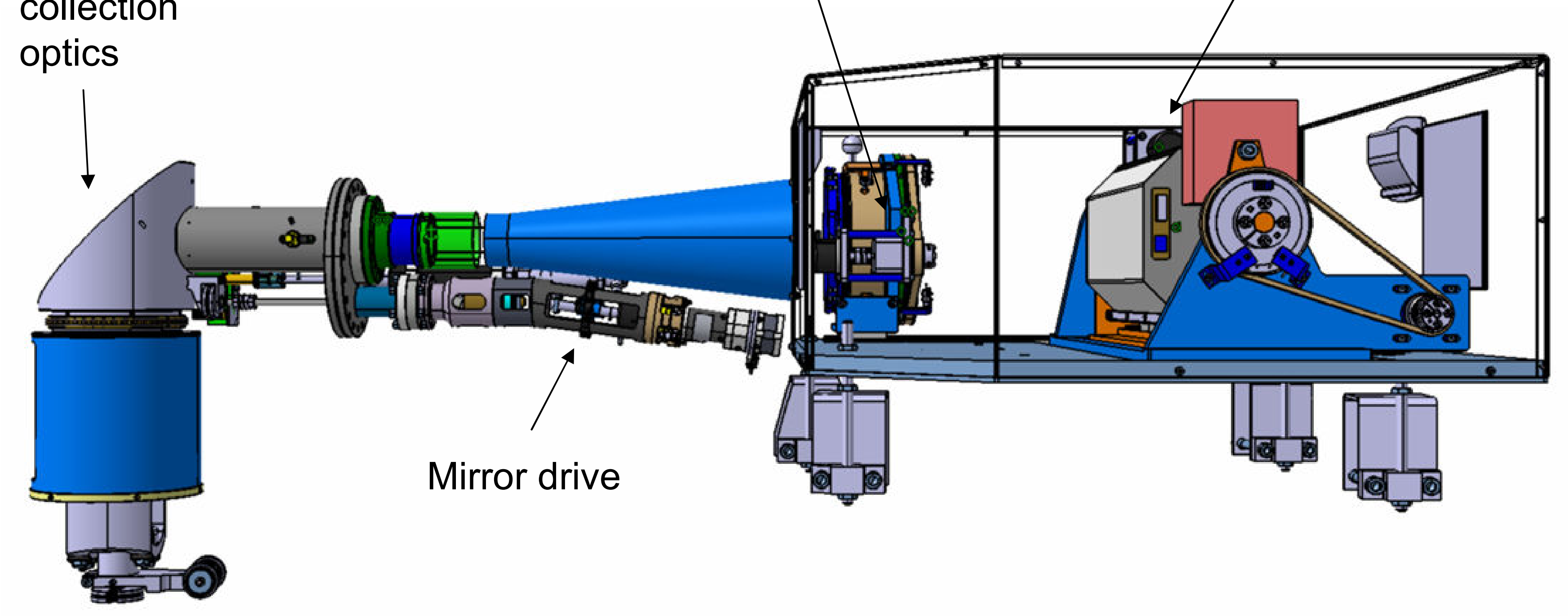

- 2D imaging of density turbulence from D_α beam emission
- APD array (8×4) camera (2 MHz) $\Delta R \sim \Delta z \sim 2$ cm for $k_{r,\theta} \leq 1.6$ cm^{-1}
- High-throughput optics for sensitivity of $\delta n_e/n_e \sim$ few × 0.1%

A. Field, S. Zoletnik et al

Stability – internal kink mode

ELM/Pedestal	Exhaust	Conf/transport	Stability	CD/profile opt.

- High resolution MSE facilitates improved understanding of performance limiting instabilities, e.g. in AT regimes with weak/reversed core magnetic shear

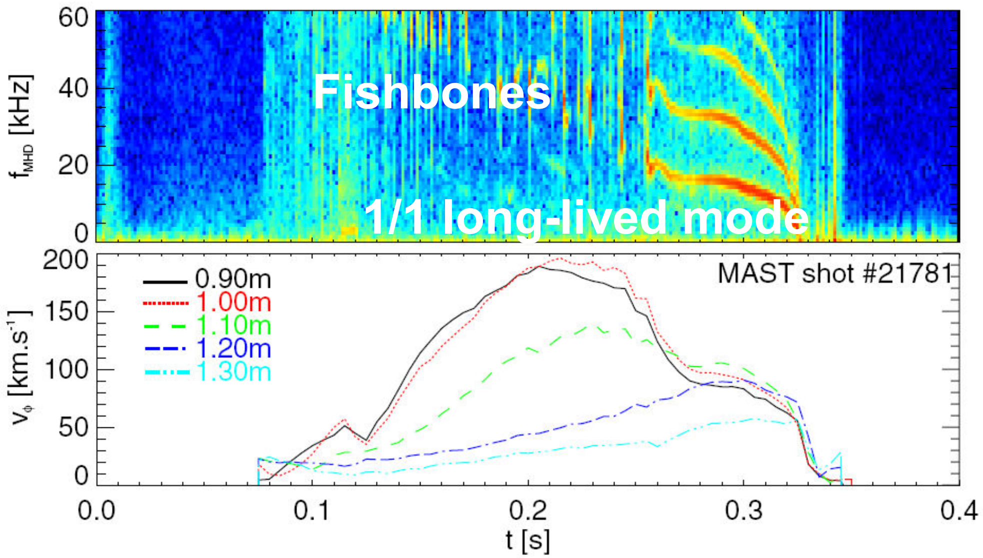

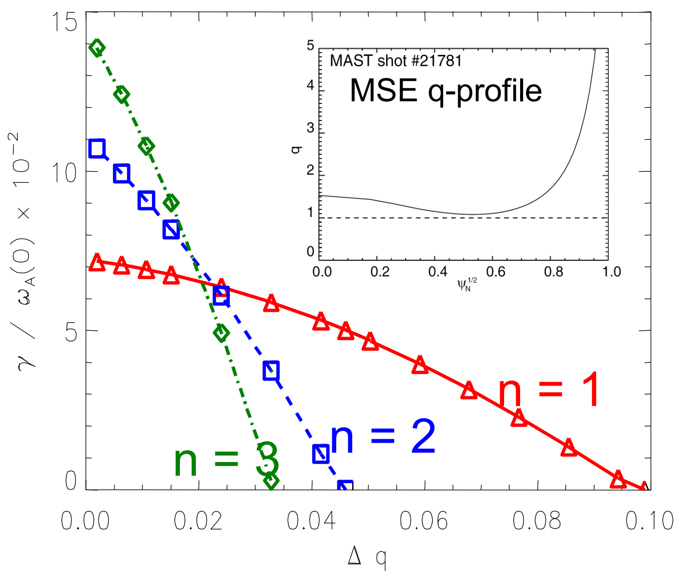

- Long-lived mode (LLM) destabilised as q→1
- Identified as n=1, internal kink mode
  - damps rotation, degrades confinement
  - expels fast ions (reducing ‘fishbone’ drive)
  - measured braking compares well with NTV theory (*M-D Hua et al PPCF 2010)*

- Higher-n modes progressively more unstable as Δq decreases
- Threshold $\Delta q = q_{min}-1$ larger in STs

I.T. Chapman et al, Nuc. Fus. 2010

NTM critical island widths

- High resolution TS system used to probe critical NTM island width, W_{Cr}
- Lasers fired in burst mode (20μs), triggered by phase locking to Mirnov signal

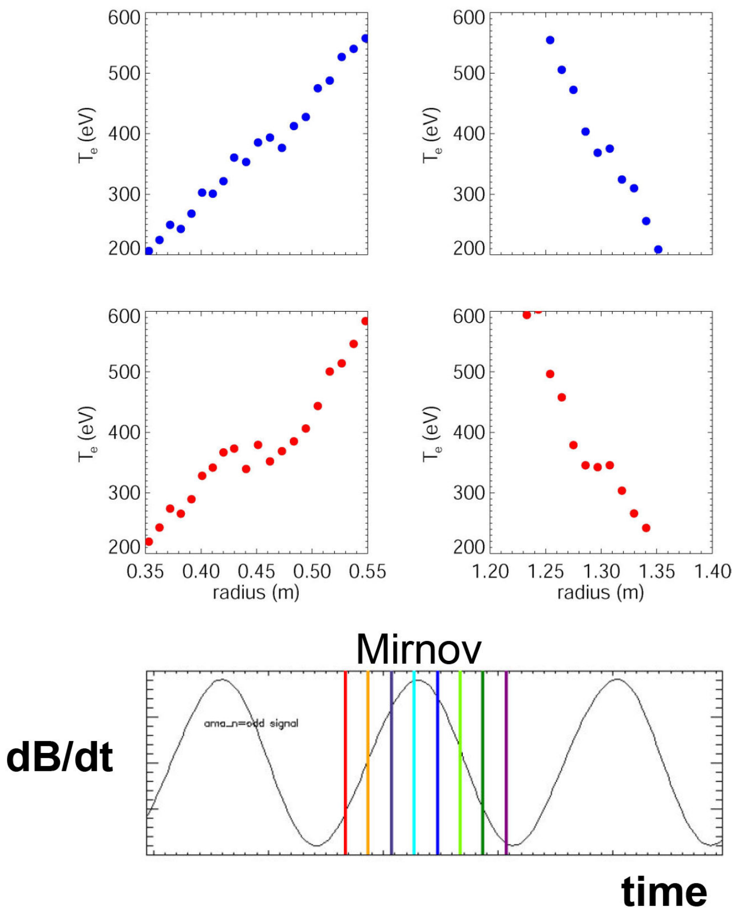

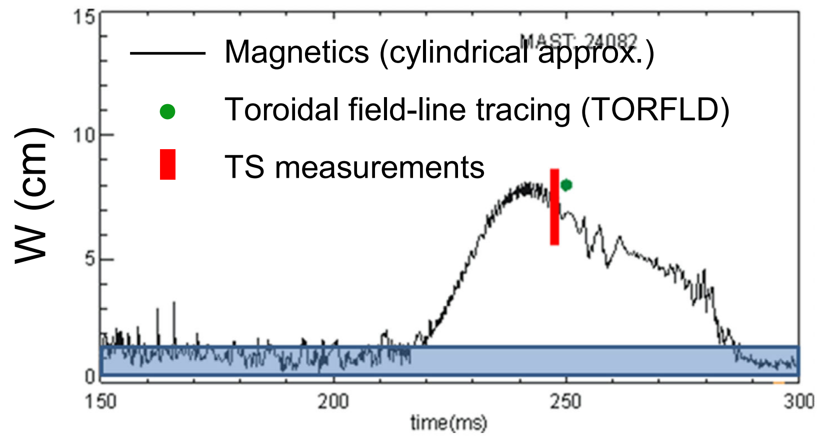

- Each pulse samples different phase of island, mapped to φ using Mirnov data
- Diffusive parallel transport model used to calculate W_{cr} (blue bar)
- Calculated W_{cr} below observed threshold
- Future work to develop full kinetic model include other threshold effects

Sawtooth crash mechanism

ELM/Pedestal	Exhaust	Conf/transport	Stability	CD/profile opt.

- Growing island structure causes increase in ∇T_e at island boundary – island observed for ~ 80μs
- Radial location of strongest ∇T_e moves to region of lower magnetic shear triggering secondary instability which explains rapid crash (<20 μs)

- Core becomes ideally MHD unstable when destabilising pressure gradient overcomes stabilising shear (ballooning or Mercier unstable depending on shaping)
- 3D modelling shows helical core is more unstable to ballooning modes than axi-symmetric modelling

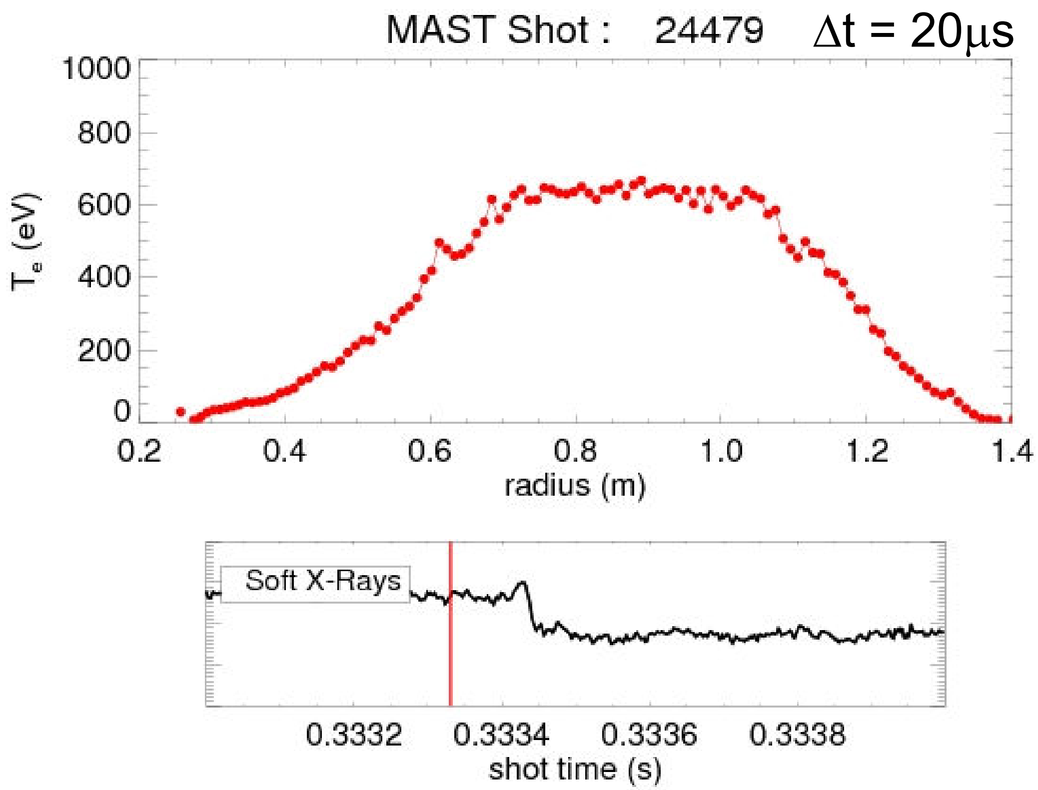

CCFE CULHAM CENTRE FOR FUSION ENERGY

Sawtooth crash mechanism

ELM/Pedestal	Exhaust	Conf/transport	Stability	CD/profile opt.

- Growing island structure causes increase in ∇T_e at island boundary – island observed for ~ 80μs
- Radial location of strongest ∇T_e moves to region of lower magnetic shear triggering secondary instability which explains rapid crash (<20 μs)
- Core becomes ideally MHD unstable when destabilising pressure gradient overcomes stabilising shear (ballooning or Mercier unstable depending on shaping)
- 3D modelling shows helical core is more unstable to ballooning modes than axi-symmetric modelling

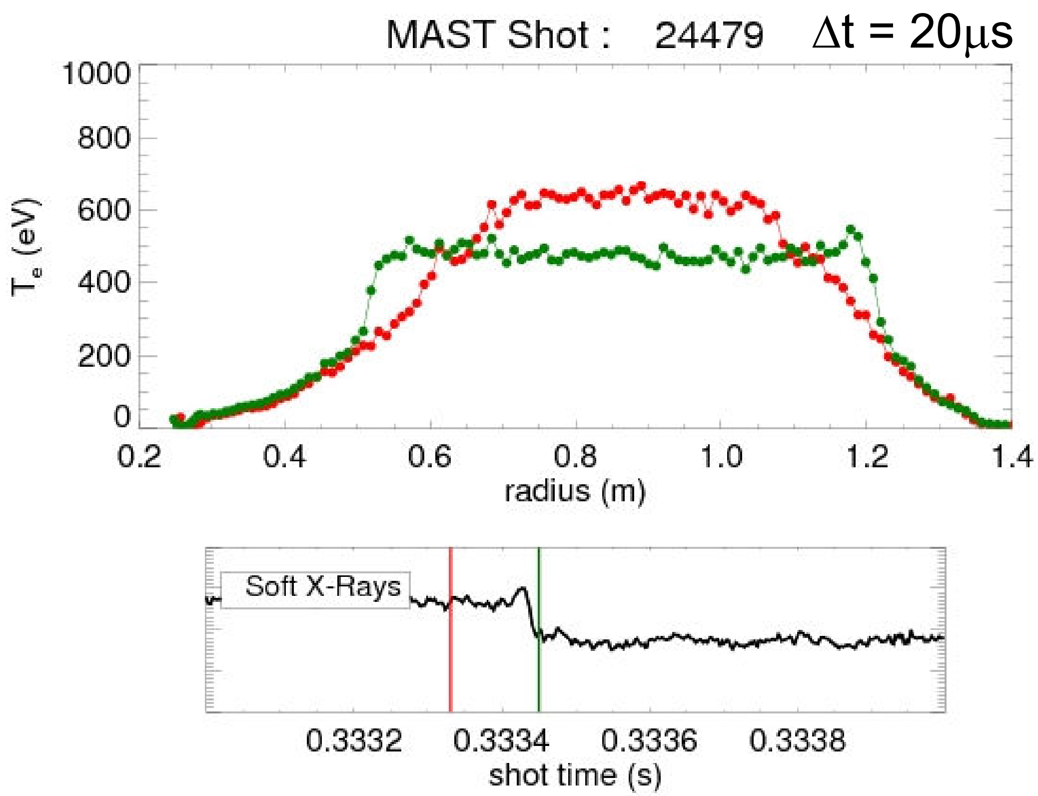

ÉCOLE POLYTECHNIQUE FÉDÉRALE DE LAUSANNE

CRPP

Fast ion physics

ELM/Pedestal	Exhaust	Conf/transport	Stability	CD/profile opt.

- Fast particle driven modes in MAST cover a broad frequency range
  - Alfvén Cascades (RSAE) → TAE ($\omega \sim v_A/2qR$) → CAE ($\omega \sim \omega_{ci}$)
- Dynamical friction (drag) shown to be important for describing non-linear wave evolution with a super-Alfvénic fast ion source
  - in MAST $v_b >> v_A$ and a good proxy for α-particles in ITER & DEMO

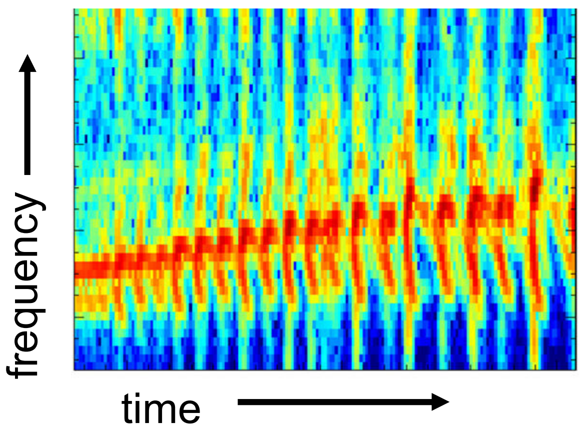

Frequency sweeping TAE in MAST #22807

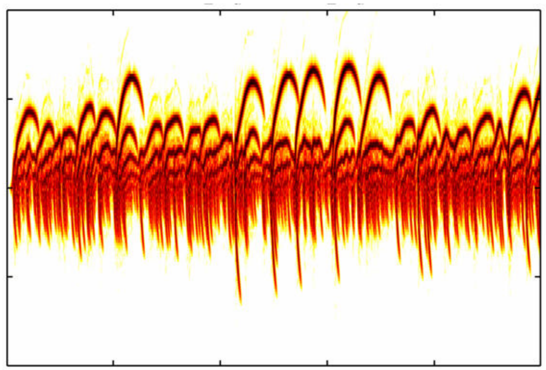

1-D bump-on-tail model

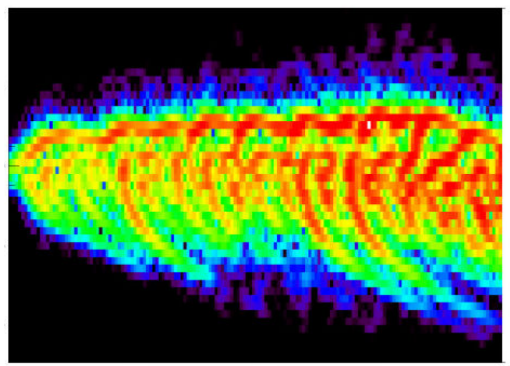

Realistic tokamak simulation of α-driven n = 3 core localized TAE using HAGIS (non-linear drift-kinetic δf code)

CHALMERS

M Lilley et al (Chalmers U.) *B Breizman et al (IFS, Texas)* *S. Pinches et al*

MAST neutron camera

ELM/Pedestal	Exhaust	Conf/transport	Stability	CD/profile opt.

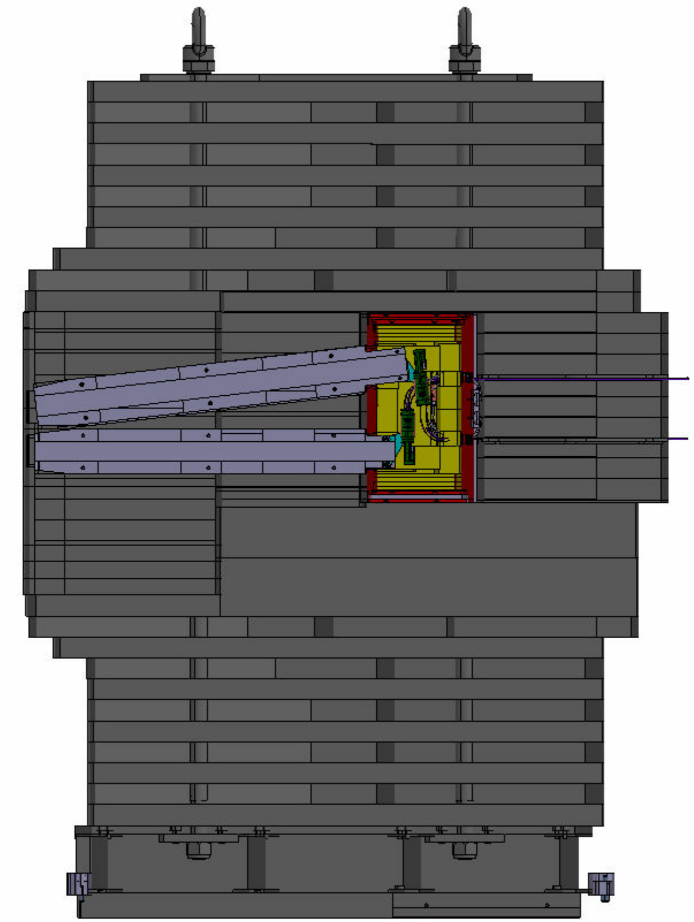

- Successfully tested in M7 (2 channels)

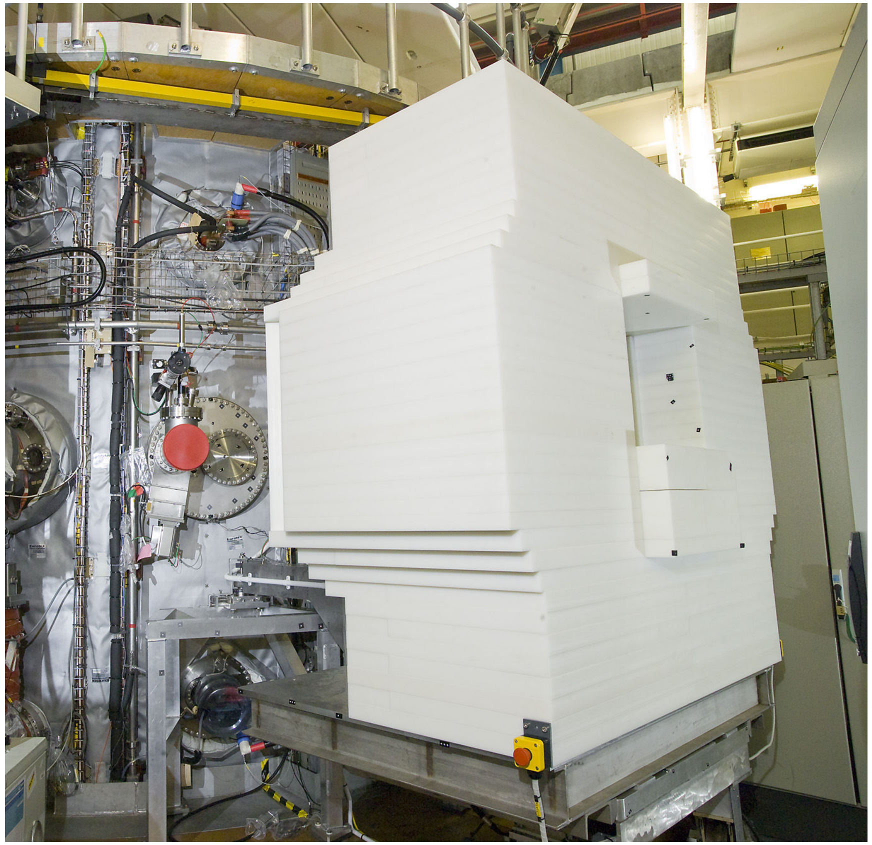

EFDA TASK

MAST neutron camera

ELM/Pedestal	Exhaust	Conf/transport	Stability	CD/profile opt.

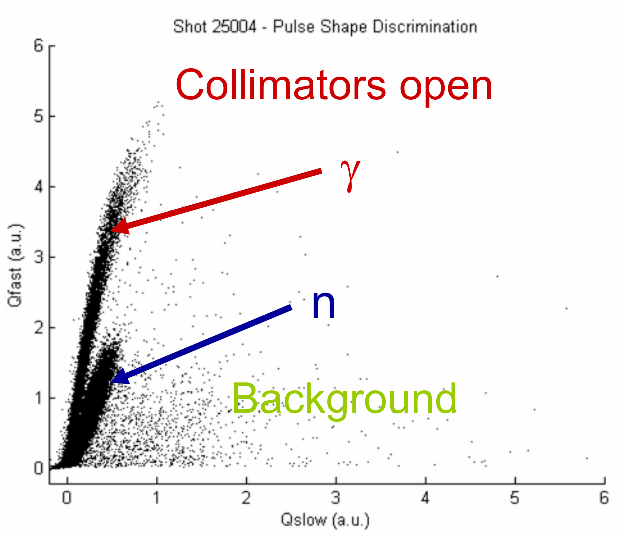

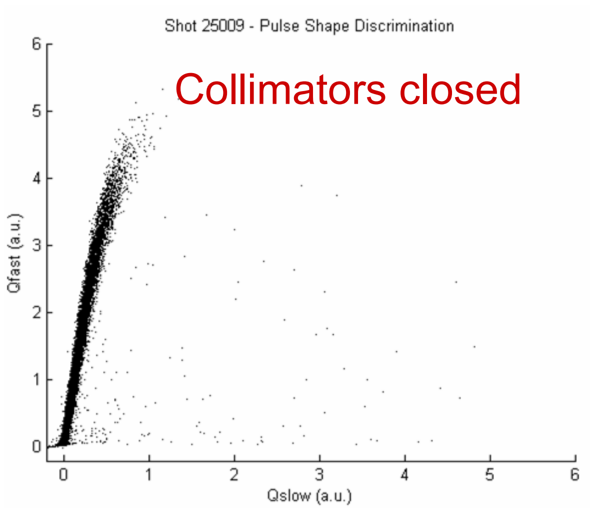

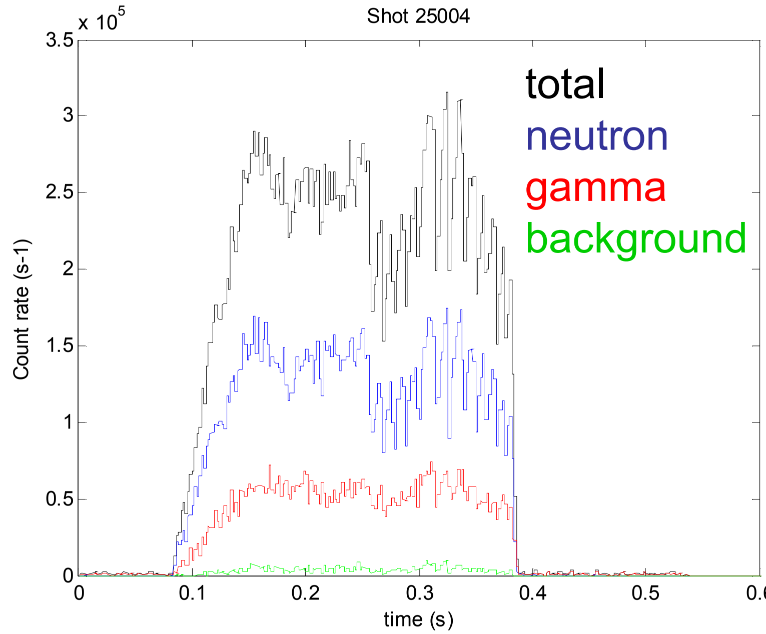

- Pulse shape discrimination between neutrons and gammas
- M8 Introduction of remotely controlled scanning capability
- Extension to 4ch and upgrade to DATAQ and detector assembly

UPPSALA UNIVERSITET

M. Cecconello et al (Uppsala U.), M. Turnyanskiy et al

Fast ion D_α spectroscopy

- Designed for *fast spectral measurements* rather than spatial resolution to follow *energy/pitch-angle distribution during fast events* e.g. fishbone instabilities
- Both vertical and toroidal views -sensitive to passing and trapped ions
- Symmetric background views to exclude background Dα emission
- Total of 32 fibres per view (~ 2 cm between channels) selected with at patch panel

Simulated FIDA spectrum

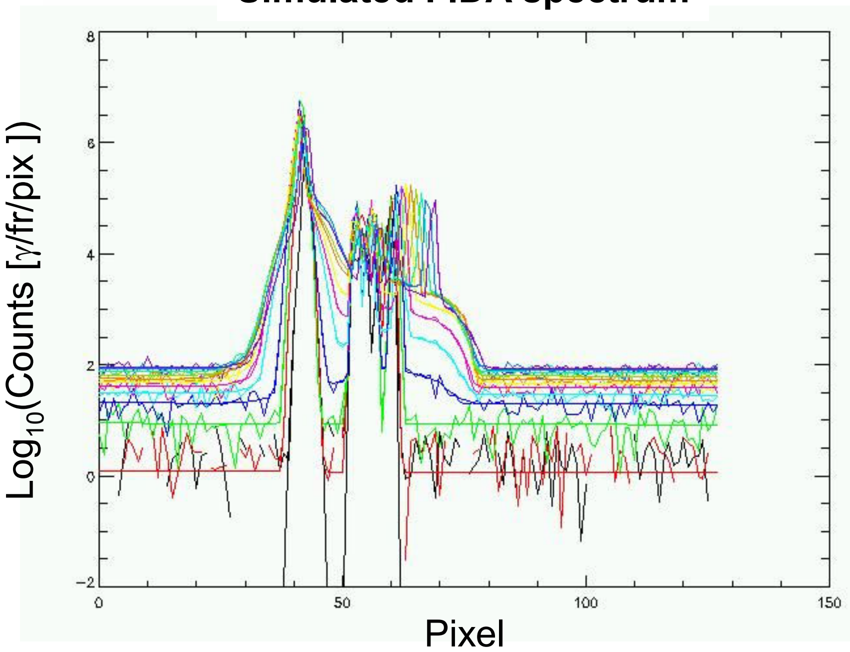

Spectrometer/Detector:

- Kaiser Optics F/1.8 imaging spectrometer with 50 or 35 mm lenses
- EEV CCD camera, 128×128 pixel chip 130 μs readout time
- 1-2 columns and 12-17 rows of chords giving 12-34 channels total
- FIDA signal of 1000 γ/fr/pix – SNR ~ 30

Advanced modelling for fast ion physics

- LOCUST charged particle tracking algorithm developed in CUDA on GPU platform

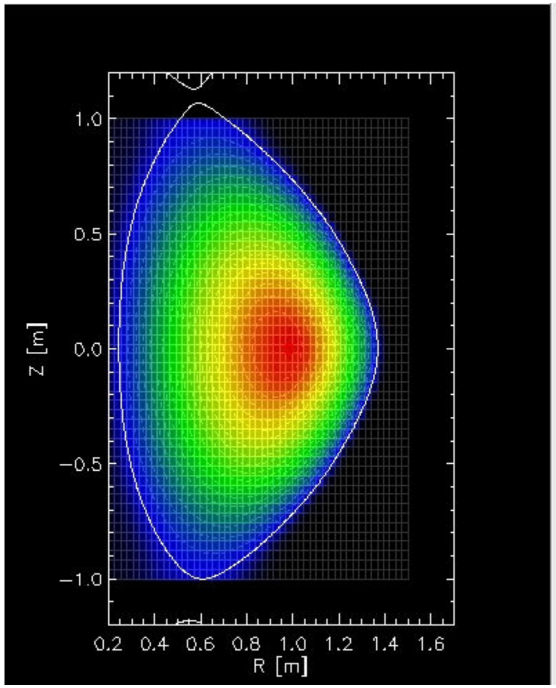

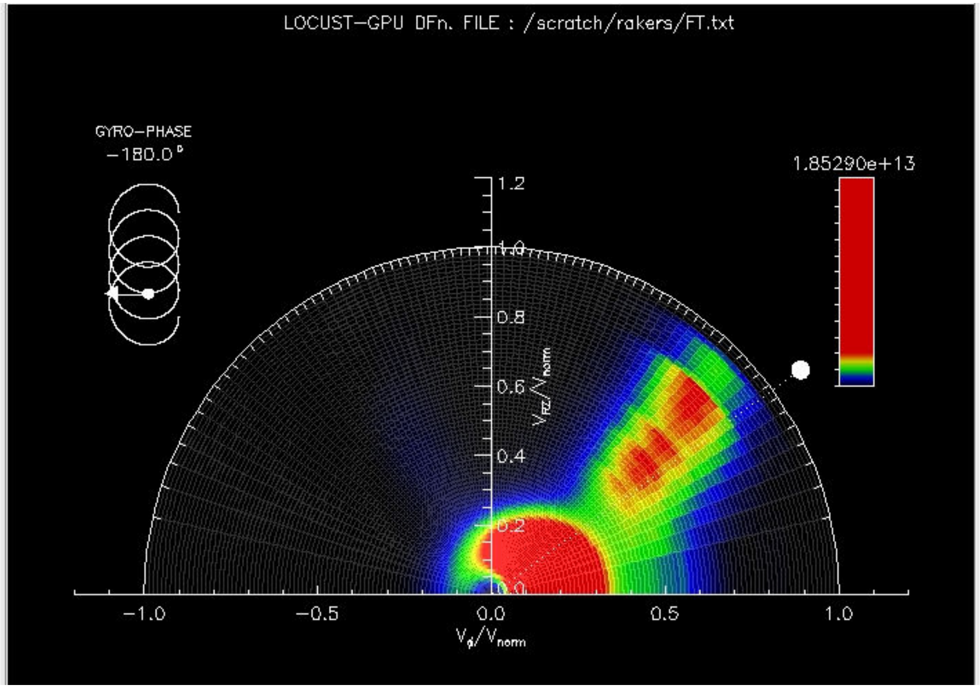

- Energy resolved 5D fusion product source distributions over all space
- Neutron camera spectra calculated as a function of chord geometry
- Smooth, gyro-phase resolved fast ion distribution function on very fine mesh
- Parallel forward tracking of fusion protons into a simulated pin-hole camera

Prototype diamond proton detector

- Detector to be tested and installed on reciprocating probe
- 2D array to be designed for implementation on MAST-Upgrade

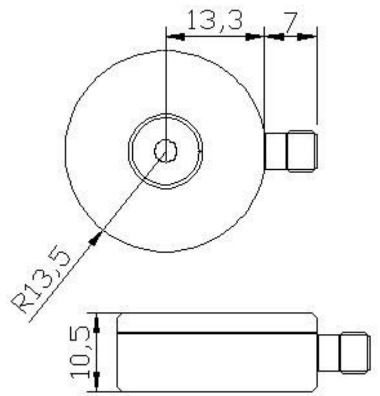

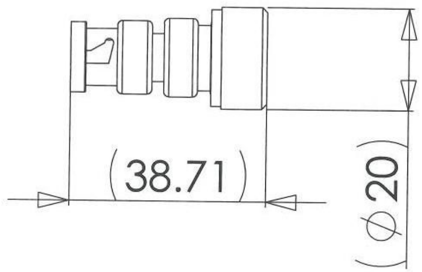

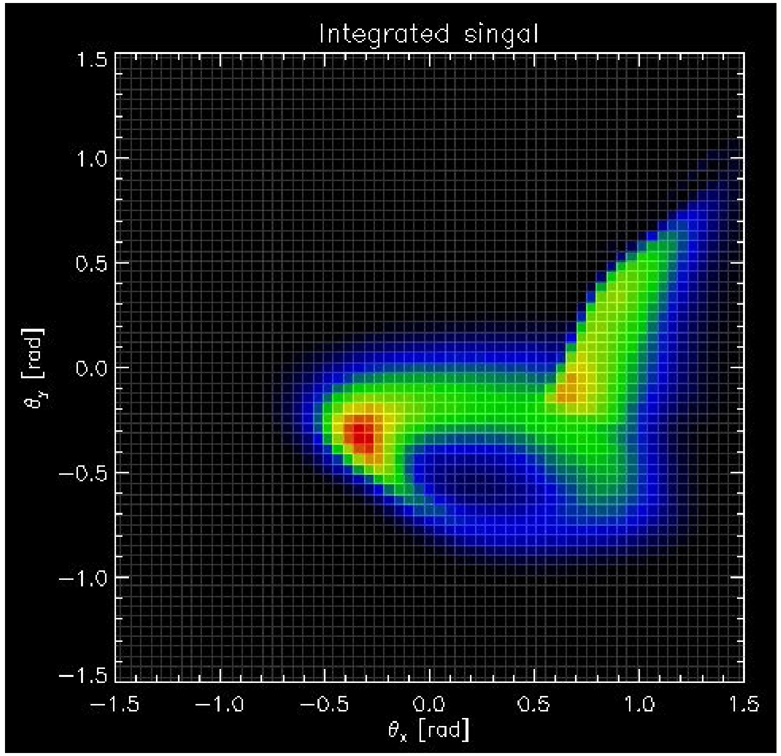

- Parallelized, forward tracking of DD fusion protons into simulated pin-hole camera performed using LOCUST-GPU

Controllable HFS gas puff

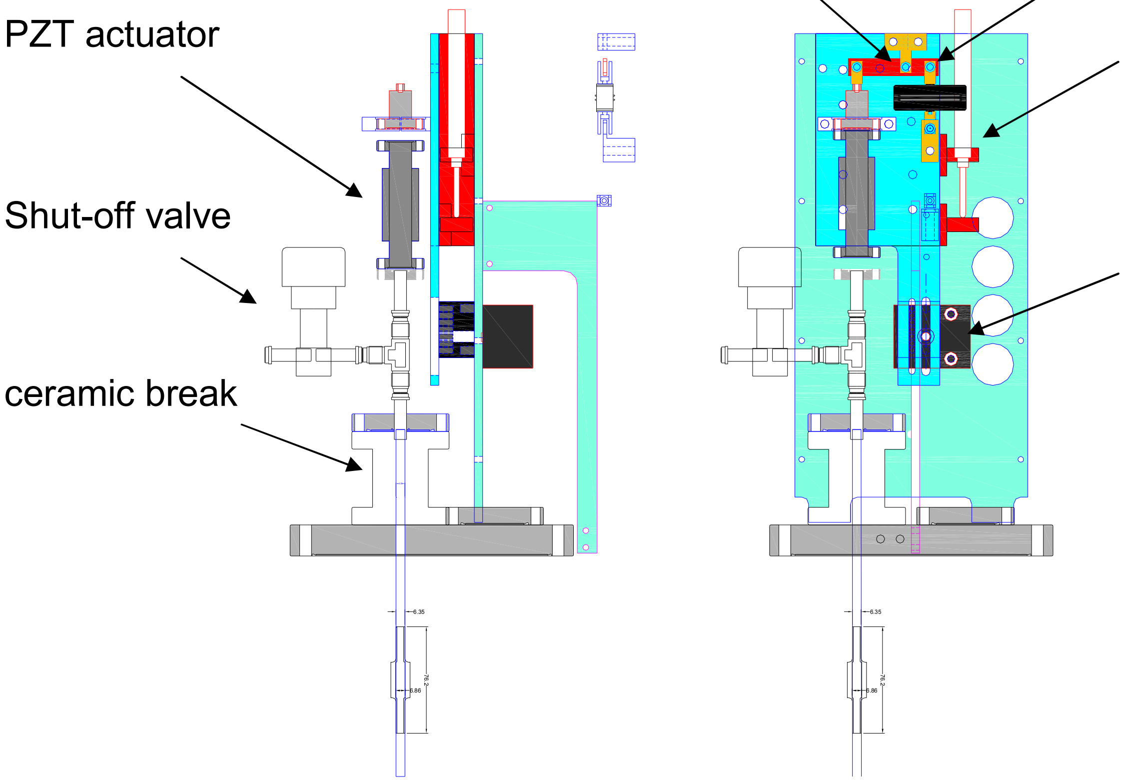

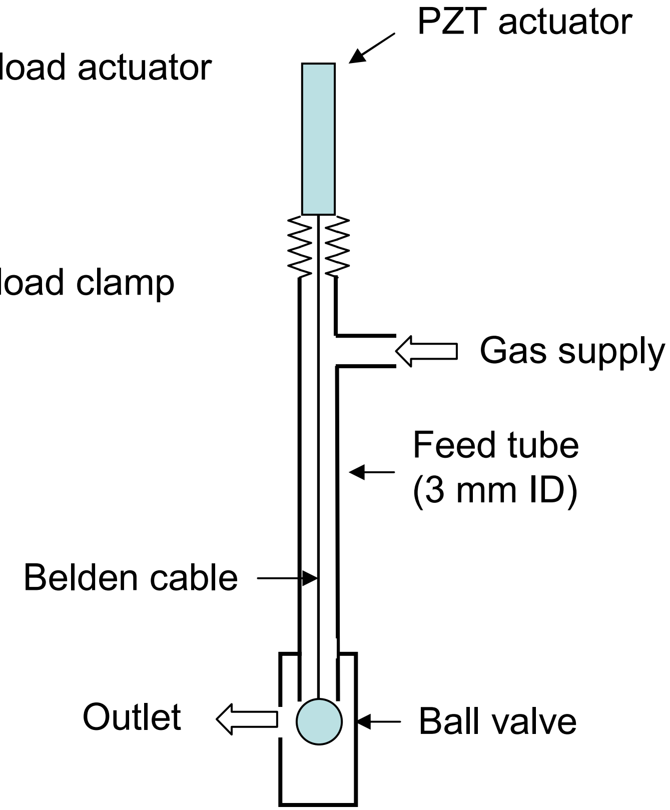

- Ball shut-off valve actuated by Belden cable though gas feed
- Piezo stack pulls on cable to choke off gas flow with ca. 200 Hz response
- Aim to fuel from HFS then shut off gas puffing for improved H-mode access

2011 Research Focus (M8)

- Physics of ELMs & their control by RMPs (incl. effects on pedestal transport, plasma screening effects etc..)

  New ELMs coils

- L-H transition & pedestal physics (focus on the underlying physics of the transition, impact of connection length and pedestal properties)

  MSE, EBW imaging, ECELESTE upgrade

- First wall/divertor heat loads (incl. toroidal asymmetries; effects of ELM control and disruption mitigation by massive gas injection; SOL width scaling; SOL T_i measurements)

  DMV, LWIR, Retarding Field Analyzers

- Transport studies – role of low-k turbulence in transport; impact of q(r) and flow shear

  2D BES, Gyro-kinetic codes

- High beta macroscopic stability incl. NTM physics (e.g. critical island widths)

  TS upgrade, ‘smart’ triggering system

- Fast particle instabilities (e.g. TAE damping); fast-ion losses/redistribution and impact on plasma performance (e.g. energy confinement, q(r) control by NBCD)

  TAE coils, FIDA, neutron camera

N.B.: May be modified by new PLs

MAST Upgrade – Stage I

- Project kick-off July 2010
- Construction 2013 - 2015